Supplement of The Cryosphere, 18, 4703–4722, 2024
https://doi.org/10.5194/tc-18-4703-2024-supplement

The Cryosphere Open Access EGU

Supplement of

Land cover succession for recently drained lakes in permafrost on the Yamal Peninsula, Western Siberia

Clemens von Baeckmann et al.

Correspondence to: Clemens von Baeckmann (clemens.von.baeckmann@bgeos.com)

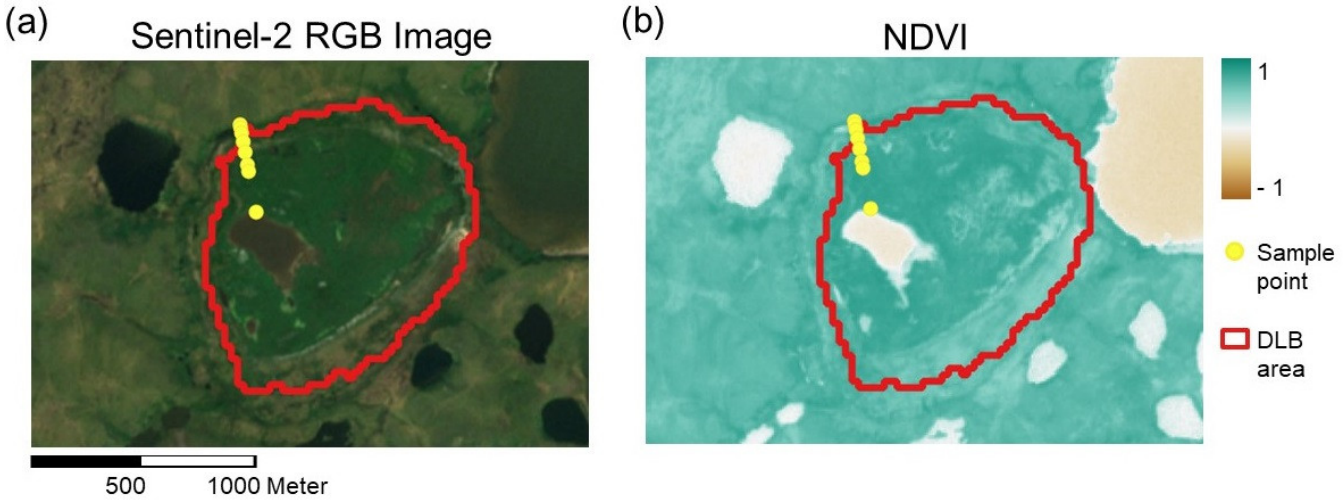

Figure S 1. Overview of collected *in situ* data (2016) at a lake located in Bioclimate subzone E drained in 2010 (a) Red, green and blue (RGB) Sentinel-2 composite for the 20.07.2016, six days before the *in situ* data were collected. (b) corresponding Normalized Difference Vegetation Index values. The lake extent in the red line is provided by the Landsat product from Nitze (2018) and refers to the maximum water area extent in 1999. For location see Figure 1 indicated as green triangle with the number 2, detailed coordinates are shown in Table A1 as well as the corresponding Landcover units are listed at the bottom of the table.

Table S 1. 'Water' fraction [%] for Drained Lake Basins separated into the two age groups and the bioclimate subzones, based on (Walker et al., 2005). The fraction is given for the quantiles: 25, 50 (median) and the 75.

	1-5 [years]			*6-10 [years]*		
Bioclimate subzone	**q25**	**q50**	**q75**	**q25**	**q50**	**q75**
B	0.00	2.42	13.78	0.00	0.13	1.24
C	0.51	3.55	16.07	0.00	0.02	1.53
D	0.34	2.78	6.56	0.00	0.86	1.69
E	1.22	6.28	14.05	0.00	0.00	1.57

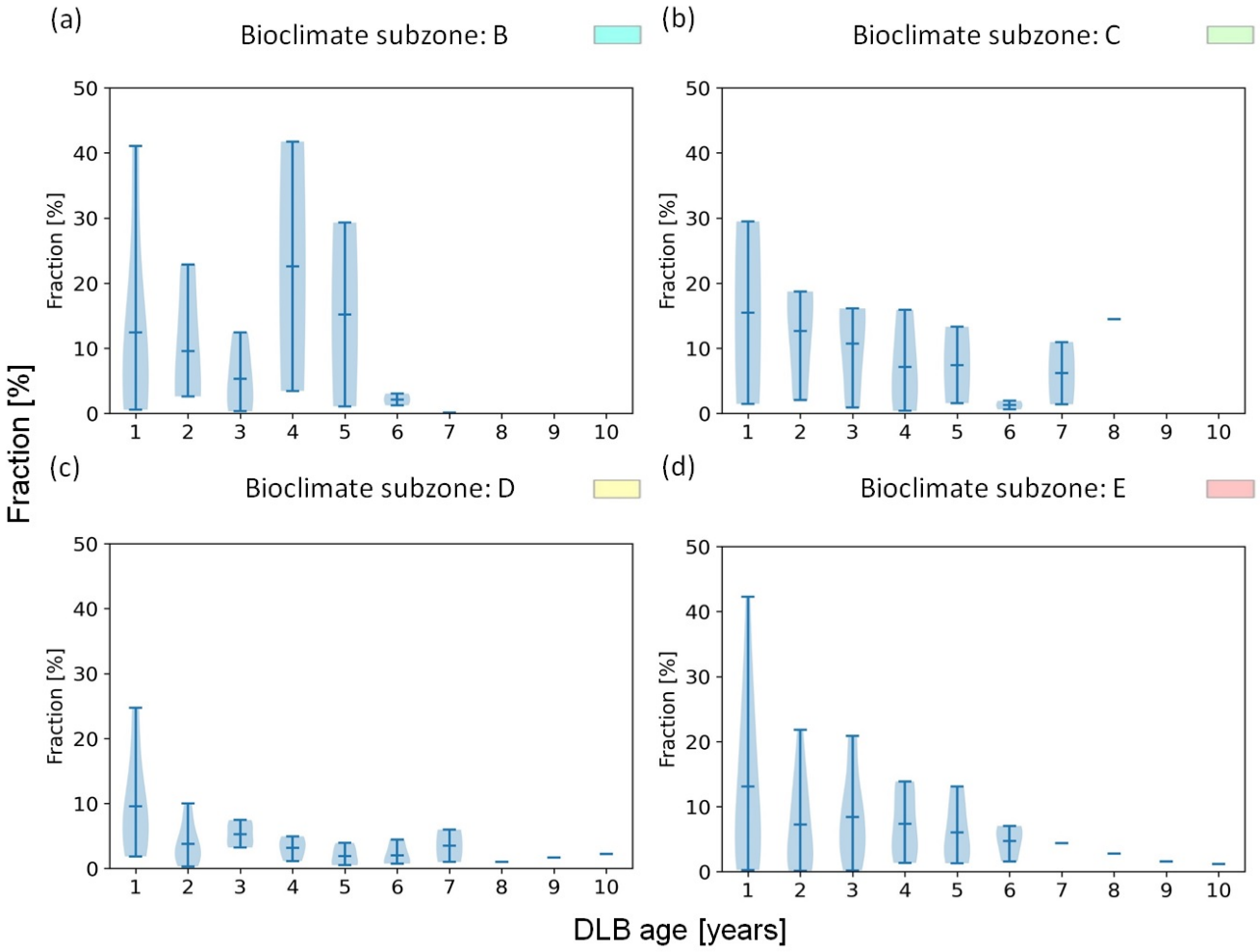

Figure S 2. Annual #1 'Water' fraction for different Drained Lake Basin ages (1-10), derived from the modified landcover classification approach using Sentinel-1 and Sentinel-2 data, based on (Bartsch et al., 2024). The data were separated into the different bioclimate subzones, based on (Walker et al., 2005).

Table S 2. Normalized Difference Vegetation Index data from Figure 2, based on Sentinel-2 satellite data. The data were separated into the different bioclimate subzones, based on (Walker et al., 2005).

Subzone	Age	Min.	q25	q50	q75	Max.
B	0	0.244	0.299	0.339	0.440	0.636
B	1	0.174	0.203	0.256	0.395	0.832
B	2	0.178	0.23	0.339	0.406	0.804
B	3	0.160	0.276	0.327	0.362	0.838
B	4	0.219	0.236	0.283	0.49	0.822
B	5	0.152	0.233	0.261	0.310	0.920
B	6	0.119	0.180	0.200	0.585	0.658
B	7	0.276	0.458	0.518	0.519	0.519
C	0	-0.039	0.143	0.326	0.362	0.399
C	1	0.140	0.183	0.225	0.296	0.367
C	2	0.202	0.25	0.299	0.336	0.373
C	3	0.202	0.208	0.235	0.304	0.435
C	4	0.200	0.216	0.312	0.357	0.438
C	5	0.226	0.279	0.333	0.465	0.596
C	6	0.000	0.192	0.384	0.474	0.564
C	7	0.453	0.473	0.494	0.528	0.562
C	8	0.253	0.349	0.445	0.478	0.512
C	9	0.000	0.250	0.500	0.565	0.631
C	10	0.318	0.418	0.519	0.619	0.719
D	0	-0.548	-0.047	0.026	0.255	0.394
D	1	-0.076	0.14	0.226	0.278	0.467
D	2	0.000	0.189	0.311	0.432	0.677
D	3	0.156	0.328	0.459	0.590	0.645
D	4	0.215	0.444	0.597	0.746	0.762
D	5	0.316	0.63	0.692	0.749	0.816
D	6	0.370	0.415	0.449	0.637	0.783
D	7	0.430	0.446	0.606	0.785	0.860
D	8	0.499	0.534	0.554	0.582	0.645
D	9	0.470	0.499	0.527	0.592	0.657
D	10	0.528	0.541	0.554	0.588	0.622
E	0	-0.211	-0.051	0.101	0.197	0.342
E	1	0.101	0.165	0.189	0.267	0.303
E	2	0.114	0.190	0.296	0.378	0.648
E	3	0.176	0.374	0.533	0.665	0.719
E	4	0.246	0.478	0.603	0.610	0.777
E	5	0.378	0.493	0.629	0.710	0.794
E	6	0.533	0.54	0.636	0.746	0.791
E	7	0.585	0.596	0.607	0.618	0.629
E	8	0.538	0.58	0.622	0.704	0.786
E	9	0.534	0.553	0.602	0.674	0.762
E	10	0.530	0.595	0.670	0.728	0.739

Table S 3. Drained Lake Basin data included in the analysis. Location and ID is derived from (Nitze, 2018). Drainage date is determined using the Landcover and Landsat products (30 m) dating back to 1984. The bioclimate subzone data were derived from (Walker et al., 2005).

ID	Subzone	Latitude	Longitude	Area [km^2]	Drainage date
60	B	73.42496079281094	70.66280500190017	0.107	2017
152	B	73.39870352619491	70.7975522861476	0.316	2015
1101	B	73.22080786365424	70.99237480663685	0.03	2016
1397	B	73.18765795505774	71.23013640235338	0.038	2016
2342	B	73.11221959595294	70.7834482074645	0.024	2016
2765	B	73.04785216110457	70.27043252486669	0.034	2019
15334	C	71.10768897791277	69.26384069338911	0.138	2019
5504	C	72.41697149803784	70.24380790390939	0.068	2018
5189	C	72.46121124669517	71.5627966727732	0.737	2012
3224	C	72.78499037075007	71.77303064621684	0.767	2012
2992	C	72.86341178148271	69.51893999696544	1.204	2018
4551	C	72.56758331586641	69.93868751526004	0.499	2013
43024	D	69.0696083304567	72.19550772080771	3.179	2008
45136	D	68.96382593086201	72.03809588636902	0.975	2015
44757	D	68.99399191150049	71.78470296267571	0.868	2019
44535	D	68.9977304827651	72.18412163847461	6.879	2017
44130	D	69.00726314342529	72.24935541980412	3.092	2017
43444	D	69.04332758055628	72.06763470084069	1.541	2019
43073	D	69.0893735586727	69.25202774779163	0.544	2020
41752	D	69.14638644377233	72.18537894738694	2.637	2014
43948	D	69.0234699279156	71.93920417439911	3.083	2021
18036	D	70.87728018214749	69.96671575233711	0.081	2016
29547	D	69.97648183379864	67.71872513449718	1.761	2015
28467	D	70.09743845627929	68.46392482356914	1.133	2008
28071	D	70.0950199842196	68.30882984224023	0.491	2012
27002	D	70.17369543135061	68.60297406124826	0.62	2017
25864	D	70.23586657005812	68.95626397721364	0.125	2019
18998	D	70.79820743092132	70.66879775349473	0.787	2019
31745	D	69.8233217077125	68.96277490728492	0.055	2020
66865	E	67.98177923184201	69.53663823249592	0.425	2007
70186	E	67.83527436585686	69.62716062115058	0.22	2017
78400	E	67.4622912423868	69.93811915306644	0.251	2008
42462	E	69.11973388904843	70.70038866061984	1.033	1998
80238	E	67.37940487721932	70.73008874630575	1.871	2016
83556	E	67.23609332608558	70.02293818188993	0.123	2017
65642	E	68.0434697280821	69.38452655569131	0.462	2012
89993	E	66.96822179973609	70.97114077757635	0.431	2019
78612	E	67.45004225716005	70.11777460022633	0.262	2019
59181	E	68.30095698084298	69.36511154390466	0.037	2019
47481	E	68.85976636255484	70.34248987389802	0.655	2019
54705	E	68.49595893530632	69.5223983537476	0.315	2019
52037	E	68.61822293555427	70.33177545034474	0.274	2011
51483	E	68.6525399397403	69.5836608444853	0.518	2018
47372	E	68.86439845532495	70.32060503706411	0.143	2017
47065	E	68.85643932518332	72.55127202246585	3.475	2016
46651	E	68.89195872910393	72.36428189115449	4.712	2019
46336	E	68.9092185090751	72.30286385025849	3.101	2019
46233	E	68.90359800248113	72.49975544764956	0.7	2019
91816	E	66.8843802526535	69.47439348834514	0.274	2020
58946	E	68.31347458615622	69.31405136414543	0.253	2004
92742	E	66.82090216288238	70.60994481629932	0.145	2019

References

Bartsch, A., Efimova, A., Widhalm, B., Muri, X., von Baeckmann, C., Bergstedt, H., Ermokhina, K., Hugelius, G., Heim, B., and Leibman, M.: Circumarctic land cover diversity considering wetness gradients, Hydrology and Earth System Sciences, 28, 2421–2481, https://doi.org/10.5194/hess-28-2421-2024, 2024.

Nitze, I.: Trends of land surface change from Landsat time-series 1999-2014, https://doi.org/10.1594/PANGAEA.884137, 2018.

Walker, D. A., Raynolds, M. K., Daniëls, F. J., Einarsson, E., Elvebakk, A., Gould, W. A., Katenin, A. E., Kholod, S. S., Markon, C. J., Melnikov, E. S., Moskalenko, N. G., Talbot, S. S., Yurtsev, B. A., and other members of the CAVM Team, T.: The Circumpolar Arctic vegetation map, Journal of Vegetation Science, 16, 267–282, https://doi.org/10.1111/j.1654-1103.2005.tb02365.x, 2005.